Simulations of X band thunderstorm airborne radar observations

Olivier Pujol, Frédéric Mesnard, Clémentine Costes, Henri Sauvageot, Nicolas Bon, Jean-Paul Artis

Simulations of X band thunderstorm airborne radar observations

Olivier Pujol [a,*], Frédéric Mesnard [b,c], Clémentine Costes [d], Henri Sauvageot [c], Nicolas Bon [d], Jean-Paul Artis [d]

[a] Université Lille 1, UFR de Physique, Laboratoire d'Optique Atmosphérique, Bât. P5, 59655 Villeneuve d'Ascq cedex, France
[b] Institut Universitaire de Technologie, GEII, 1 rue Lautréamont, 65016, Tarbes, France
[c] Université Toulouse III, Laboratoire d'Aérologie, 14 avenue Édouard Belin, 31400, Toulouse, France
[d] Thalès Systèmes Aéroportés, 10 avenue de la 1ere D. F. L, 29200, Brest, France

This paper deals with simulations of thunderstorm airborne radar observations at X band ($f = 10$ GHz), the frequency used by the meteorological radars of civil aviation. For this study, a radar simulator using NEXRAD data is elaborated. The various problems affecting X band (attenuation and non Rayleigh scattering) can lead to an underestimation or a false estimation of hazards. They are illustrated by a real case of severe tornadic storm in Oklahoma. It is shown that the first Mie mode of hailstones limits the large hail area detection because hail can be mistaken with non dangerous heavy rain. In addition, the problem commonly encountered with a large radar beam aperture and for long distance of observations is addressed. Ground clutter is shown to contaminate the signal of reflectivity.

1. Introduction

Thunderstorms are the most dangerous convective systems in the atmosphere. Their large vertical extension and their extreme intensity in terms of air motion and precipitation are a serious problem for civil aviation (e.g. Houze 1993; Mahapatra 1999). At tropical latitudes, thunderstorm clusters in the form of mesoscale convective systems like squall lines, covering several thousands of square kilometres, can raise problems for pilots. Indeed, for obvious security reasons, a pilot must identify as soon as possible such dangerous meteorological targets; it means that thunderstorms, isolated or organized in a mesoscale structure, have to be located as precisely as possible at distances greater than 100 km. For a plane with a velocity of 800 km h^{-1}, a thunderstorm at a distance of 100 km is reached in less than 8 minutes! To quantify the hazard, avoid isolated thunderstorms, or find a no dangerous passing through inside a mesoscale convective system, X band radars are used since they present the advantage of having an antenna small enough to be set in the radome of the plane. However, in this frequency domain ($f = 10$ GHz, wavelength $\lambda \approx 3.2$ cm), cloud and precipitation attenuation is significant (e.g. Gosset and Sauvageot, 1992). In addition, owing to the large antenna beam aperture, the poor space resolution jeopardizes the correct identification and location of individual convective cells because, at a long distance, beamwidth can be larger than the target.

It is thus important to know what X band radars would really see and consequently indicate to pilots. In this paper, a radar simulator is elaborated and X band radar observations are simulated in order to point out the main problems that can be encountered with such radars in relation to hazard detection.

For the sake of clarity, this work is limited to a static mode, i.e. the situation of a plane looking at a severe precipitating system at a given time is considered.

This work is devoted to highlighting difficulties of airborne meteorological radar applied to civil aviation. First,

* Corresponding author.
E-mail addresses: olivier.pujol@loa.univ-lille1.fr (O. Pujol), mesf@aero.obs-mip.fr (F. Mesnard), clementine.costes@fr.thalesgroup.com (C. Costes), sauh@aero.obs-mip.fr (H. Sauvageot), nicolas.bon@fr.thalesgroup.com (N. Bon), jean-paul.artis@fr.thalesgroup.com (J.-P. Artis).

Table 1
Order of magnitude of various hydrometeor physical characteristics.

Hydrometeor	D_{min} (mm)	D_{max} (mm)	ρ (g cm^{-3})
Ice crystals	0.1	2	0.1–0.9
Snow	1	5	<0.2
Graupels	0.5	5	0.2–0.8
Hail	5	50	>0.8
Rain	0.5	5	1
Cloud droplets	1 μm	50 μm	1

D is equivalent spherical diameter and ρ density (Pruppacher and Klett, 1997; Glickman, 2000).

some theoretical considerations about reflectivity factor at X band are briefly presented. Then, a real situation, coming from the US NEXRAD database, is presented and serves as an example to illustrate the problems that can arise from X band airborne radar observations at long distance. For that, the radar simulator elaborated is described. The final section concludes and indicates directions for further studies.

2. Theoretical considerations about X band

Thunderstorm structure consists of an intense convective cell embedded in a stratiform like background (e.g. Houze, 1993), made up of various hydrometeors whose physical characteristics are summarized in Table 1 (Pruppacher and Klett, 1997; Glickman, 2000). For civil aviation, the largest and heaviest precipitating particles, the most dangerous ones for a plane, are hailstones. They can cause much impressive damage, which is why a pilot must identify hail areas as soon as possible in order to avoid them.

Hail area identification with a X band radar can be problematic because the first Mie mode occurs for hailstone diameters D_h around 1.5 cm (Atlas and Ludlam, 1961; Doviak and Zrnic, 2006; Sauvageot, 1992, p. 135). For such hailstones, equivalent reflectivity factor Z_e is about 70 dBZ at S band and 52 dBZ at X band. The equivalent reflectivity factor of hail is smaller at X band than at S band. Because of this relatively low reflectivity, large hailstones, with diameter close and higher than 4 cm, can be confused with heavy rain.

Another problem implying an underestimation of hazards is due to hydrometeor attenuation. Many empirical relationships have been proposed to correct attenuation by precipitation, especially for rain. However, as underlined by Pujol et al. (2007a), tiny droplets of non precipitating clouds are a non negligible source of attenuation, although they are undetectable by radars. Cloud attenuation is proportional to cloud liquid water content M_c (e.g. Gosset and Sauvageot, 1992, Gaussiat et al., 2003). For X band and $M_c = 1$ g m^{-3}, at a temperature of 0 °C, for a propagation through a cloud of 50 km, the two way attenuation is about 10 dB. Consequently, reflectivity fields are degraded by undetected in reflectivity cloud components. For ice cloud, attenuation is negligible (e.g. Hogan et al., 2000).

3. Data and system description

The US NEXRAD database provided the case used to illustrate the problems linked with a X band airborne radar with large aperture. The real case considered is a tornadic storm (e.g. Klemp, 1987) occurring during the night between

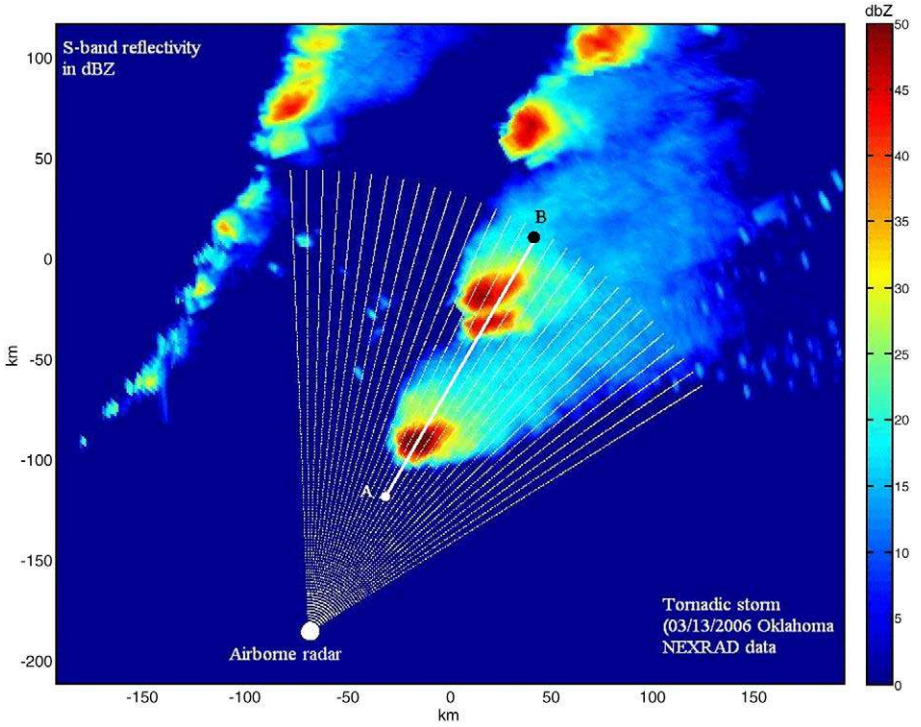

Fig. 1. S band horizontal reflectivity cross section at a height of 10 km AGL for March 13, 2006 tornado in Oklahoma at 03:44 UT (data originating from the NEXRAD database). The white point shows the location of the radar and the white solid lines represent azimuth directions.

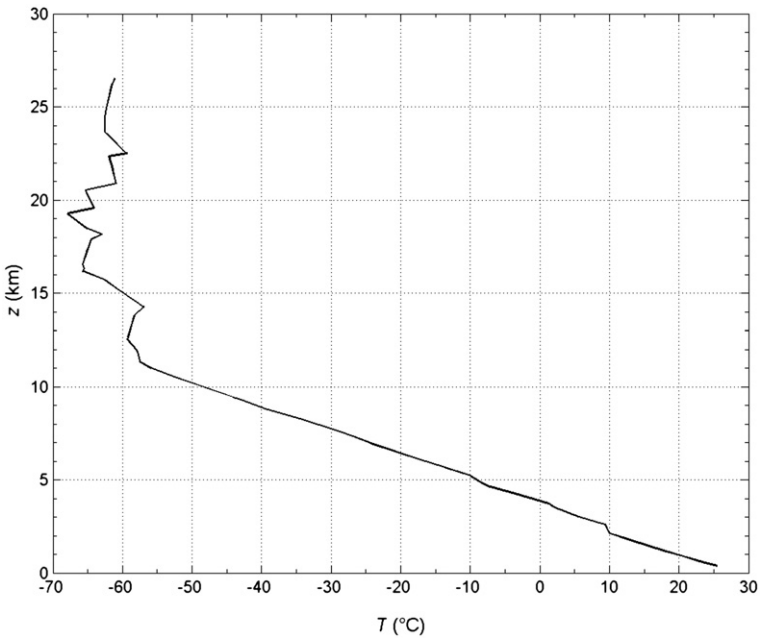

Fig. 2. Vertical profile of temperature from the radiosounding of Sprinfied at 00:00 UT on March 13, 2006, near Leach (Oklahoma).

March 12 and 13, 2006 in the region of Leach (36°,10′N; 94°,55′W) in Oklahoma. According to the description given by the NEXRAD database website, the tornadic storm produced heavy hailstones which caused damages and injured eight persons. The intense precipitating system was made of several convective cells, aligned along a southwest northeast direction (Fig. 1), with a vertical extension of 16 km AGL (above ground level). The reflectivity was greater than 50 dBZ and up to 70 dBZ at low levels (below 7 km AGL) in some places (not shown). The system moved eastward and regenerated in the west in the form of another banded structure. In the present work, where only the static mode is considered, the situation of the storm at 03:44 UT in the morning is used.

Another important data is the temperature field which is assumed to be provided by the radiosounding at 00:00 UT on March 13, 2006 of the Springfield station located at 37°,22′ N, 93°,40′ W and 390 m above mean sea level (MSL). Temperature vertical profile (Fig. 2) shows a 0 °C level around 3.8 km above MSL. In addition, one can estimate tropopause altitude to be 16–18 km.

4. Simulation of X band observations

A radar observation simulator is an analytical tool for computing radar reflectivity and attenuation fields of a given meteorological target for various radar characteristics. The literature is rich of examples of radar simulators (Vivekanandan et al., 1993; Giuli et al., 1994; Anagnostou and Krajewski, 1997; Capsoni et al., 2001; Haase and Crewell, 2000; Féral et al., 2003a,b; Pujol et al., 2007a,b). The meteorological target can be built by means of hydrometeor size distributions, for example to study cloud droplet attenuation at different wavelengths (Pujol et al., 2007a) and the influence of drizzle on liquid water content retrievals for warm clouds at S band (Pujol et al., 2007b). Observed data can also be considered as input data of the radar simulator.

This section illustrates, by means of radar simulations and using the data described in Section 3, the various problems encountered by a X band radar when observing a convective storm at long distance (r>100 km), with a large beamwidth (between half power points) of $\theta_{3\ \mathrm{dB}}=3°$. The other important radar technical characteristics used for simulation are listed in Table 2. These values are typical of airborne radar. An interesting and common configuration for pilots occurs when the plane is aligned with several convective cells. For example, the configuration represented in Fig. 1 may be considered, where the radar spots on a line of three convective cells, whose reflectivity is greater than 40 dBZ, even at an height of 10 km AGL. The closest convective cell is about 100 km away from the radar, while the second and third ones are located at a distance of 180 km. This situation is clearly dangerous for the plane and the pilot must change his route.

Table 2
Radar technical characteristics used for simulation.

Radar characteristics	
Wavelength	3.2 cm
Polarization	Vertical
Pulse duration/radial resolution	4.8 μs/1440 m
Peak power	36 W
Antenna beam pattern	Gaussian
Beamwidth (3 dB)	3°
Radar sensitivity	16 dBZ to 100 km/22 dBZ to 200 km
Thermal noise mean power	−119.3 dBm

Table 3
Hydrometeor identification for convective system (a) and stratiform one (b) through S band reflectivity factor $Z_{e,S}$ and temperature T, and corresponding relation for conversion of $Z_{e,S}$ to physical parameters (e.g., Sauvageot, 1992).

(a) Convective profile

$T>0$ °C	$Z_{e,S}<55$ dBZ	Rain	$Z_{e,S}=300\ R^{1.4}$
	$Z_{e,S}\geq 55$ dBZ	Hail	$Z_{e,S}=1.5\times10^{4}\ R^{1.2}$
$T<0$ °C	$Z_{e,S}<10$ dBZ	Ice crystals	$Z_{e,S}=900\ (IWC)^2$
	10 dBZ$\leq Z_{e,S}\leq$47 dBZ	Snow	$Z_{e,S}=1000\ R^{1.6}$
	$Z_{e,S}\geq 47$ dBZ	Hail	Same as above

(b) Stratiform profile

$T>0$ °C	All values of $Z_{e,S}$	Rain	$Z_{e,S}=250\ R^{1.5}$
0 °C$<T<-40$ °C	$Z_{e,S}>10$ dBZ	Snow	Same relation as in (a)
	$Z_{e,S}<10$ dBZ	Ice crystals	Same relation as in (a)
$T<-40$ °C		Ice crystals	Same relation as in (a)

For rain, similar Z–R relations by Nzeukou et al. (2004) can also be used. On the right, $Z_{e,S}$ is expressed in mm^6 m^{-3}, fall rate R in mm h^{-1} and ice water content IWC in g m^{-3}. Note that hail is considered to be dry hail. Fall rate for hail and snow is equivalent rainfall rate of melted hailstones and snowflakes.

Table 4
Relation for conversion of physical parameters to reflectivity factor $Z_{e,X}$ and attenuation A at X band (e.g., Sauvageot, 1992).

Hydrometeor	Reflectivity factor	Attenuation
Cloud droplets	$Z_{e,x}=0.026\ (LWC)^{1.61}$	$A=0.01\times(-0.23\ T+10)\ LWC^2$
Ice crystals	$Z_{e,x}=900\ (IWC)^2$	$6\times10^{-4}\ IWC$
Rain	$Z_{e,x}=275\ R^{1.48}$	$0.01\ R^{1.2}$
Snow	$Z_{e,x}=500\ R^{1.6}$	$(3.3\ R^2+2\ R)\times10^{-4}$
Hail	$Z_{e,x}=8000\ R$	$0.01\ R^{1.2}$

Reflectivity is in mm^6 m^{-3}, attenuation in dB km^{-1}, R in mm h^{-1}, and LWC and IWC in g m^{-3}.

4.1. Methodology for simulations of X band radar observations

The methodology of the radar simulator is made of five main parts. The first step is to discriminate from S band reflectivity factor, $Z_{e,S}$, convective profiles from stratiform ones. For that, one can use, for instance, the value of reflectivity at 1500 m above the 0 °C level (i.e., at an altitude of about 5.3 km) which should be greater than 30 dBZ for a convective profile (Smyth and Illingworth, 1998). Vertically integrated liquid water, available with NEXRAD data level III, is also a good indicator of convective zones with heavy rainfall and hail areas. In a second step, using $Z_{e,S}$ and the vertical profile of temperature, the different hydrometeors are identified according to the convective stratiform discrimination performed at step 1. Details of hydrometeor identification is given in the third column of the Table 3. It has to be noted that cloud droplets have been added to precipitation by using temperature through a relation we have developped from microwave radiometric profiler observations (to be published), $\log(LWC/1.68)=0.027\ T-0.88$, where LWC is liquid water content (in g m^{-3}), log denotes decimal logarithm and the factor 1.68 takes into account the fact that LWC field is more extended than precipitation field. One can use as well the relation of Pujol et al. (2007b) which relies cloud droplet reflectivity factor to LWC at S band, $Z_{e,S}=0.026\ LWC^{1.61}$. The step 3 consists in converting, for each identified hydrometeor, $Z_{e,S}$ to physical parameters as precipitation rate R or water content, through the various relations explicited in the fourth column of the Table 3. In a fourth step, these physical parameters are then converted to reflectivity factor $Z_{e,X}$ and attenuation A at X band using the relations listed in the Table 4. Finally, using the previously obtained $Z_{e,X}$ and A fields, a radar observation is simulated by considering all the characteristics of the predefined radar, in particular by making a convolution of the $Z_{e,X}$ and A fields by the antenna mean beam pattern which is chosen to have a Gaussian form and no side lobes. For a given point M (r, θ, φ) at a distance r far from the radar, θ and φ being the antenna direction of the radar, attenuated X band reflectivity factor is first computed by subtracting twice the attenuation values along the radar pointing direction (between the radar and M) from $Z_{e,X}$. Attenuated reflectivity is then weighted by the antenna beam pattern and weighted values are summed to obtain the measured reflectivity at X band at M. We proceed identically for the next antenna pointing which differs from the previous one by $\Delta\theta=0.7°$ and $\Delta\varphi=2°$. The simulation finishes when the whole meteorological target has been covered.

An important feature of the radar simulator is ground clutter which must be computed when the radar beam intercepts a plane surface S_r of the ground. Backscattering cross section σ of the ground can be correctly estimated by

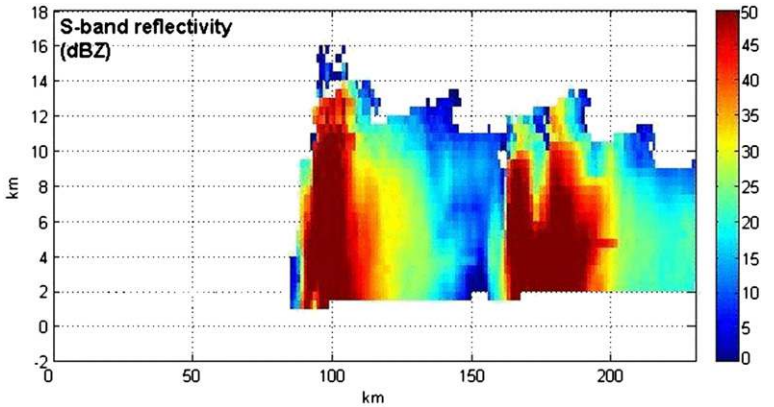

Fig. 3. Vertical S band reflectivity cross section along the line AB line of Fig. 1. Altitudes are above ground level.

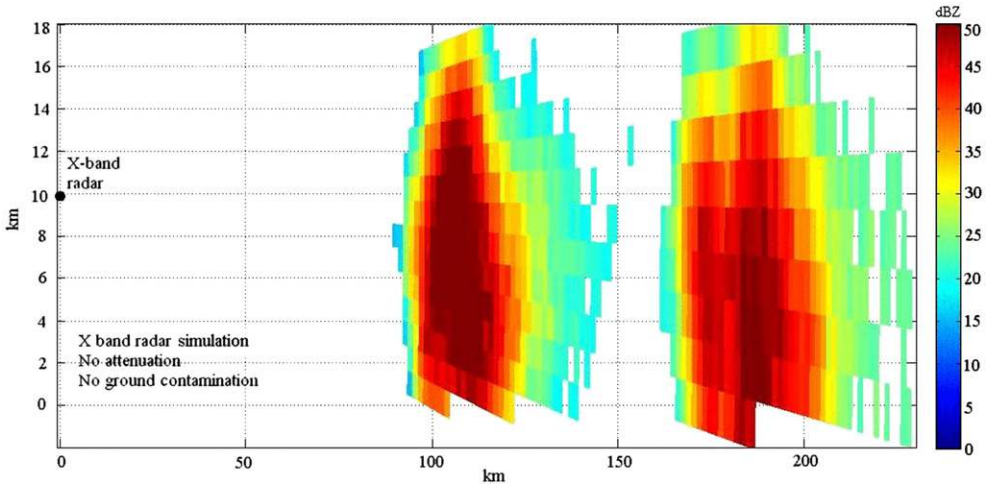

Fig. 4. Vertical cross section along AB line of a X band simulated radar observation without considering hydrometeor attenuation and ground clutter. Altitudes are above ground level.

the relation $\sigma = \Gamma \sin(\alpha)\ S_r$ (Nathanson, 1969), with $\Gamma = 0.184\ \mathrm{m}^2\ \mathrm{m}^{-2}$ and α the grazing angle (in degrees). Such a ground clutter can correspond to grass, beach, marshland, lakes, etc. It is worth noting that ground clutter is important when operating at long distances with a large beam aperture (3°): at 200 km, the vertical extension of the radar beam is 10 km, so that it intercepts the ground and approximately a complete convective cumulonimbus cell.

4.2. Results of simulations

Fig. 3 displays a vertical cross section of the S band reflectivity field along the AB line of Fig. 1. Convective cells have reflectivities higher than 40 dBZ up to about 13 km of height AGL. Horizontal extension of the convective cells is around 20 km. The cells are embedded in a stratiform background of reflectivity lower than 30 dBZ.

Figs. 4, 5, and 6 sketch vertical cross sections of the simulated X band radar observations along the same AB section than the one represented in Fig. 1. Fig. 4 is relative to the X band observation when hydrometeor attenuation and ground clutter are not considered. Two convective cells can be observed with a top reaching a height of 18 km AGL and with reflectivity greater than 40 dBZ up to a height of 14 km AGL. These cells are separated from each other by about 50 km and embedded in a stratiform background characterized by a reflectivity lower than 30 dBZ. Fig. 5 is the same as Fig. 4 except that hydrometeor attenuation is taken into account; ground clutter is still not considered in the simulation. One can notice the strong degradation of the reflectivity field with the distance. The second cell notably presents a reflectivity lower than 35 dBZ due to the strong attenuation by the first cell. The latter is also strongly attenuated in its farthest part. In the front side of

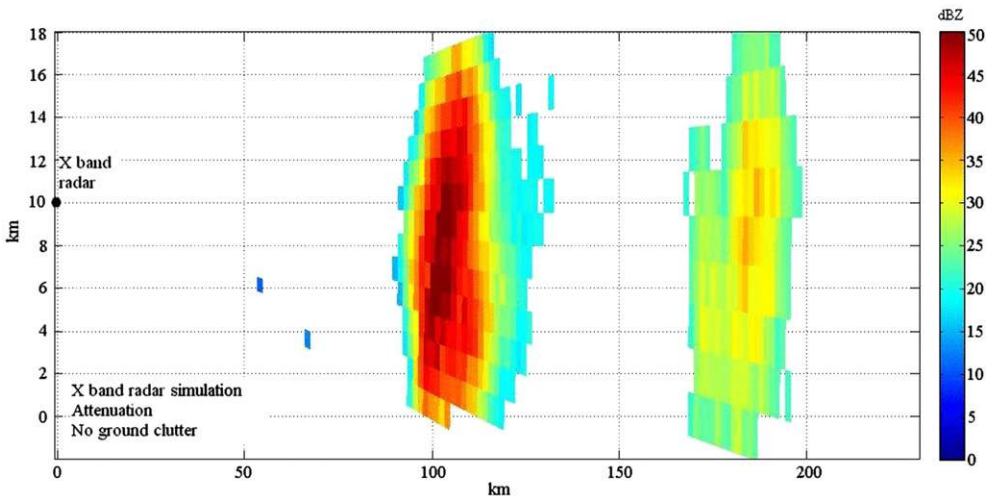

Fig. 5. Same as Fig. 4 taking into account cloud and precipitation attenuation.

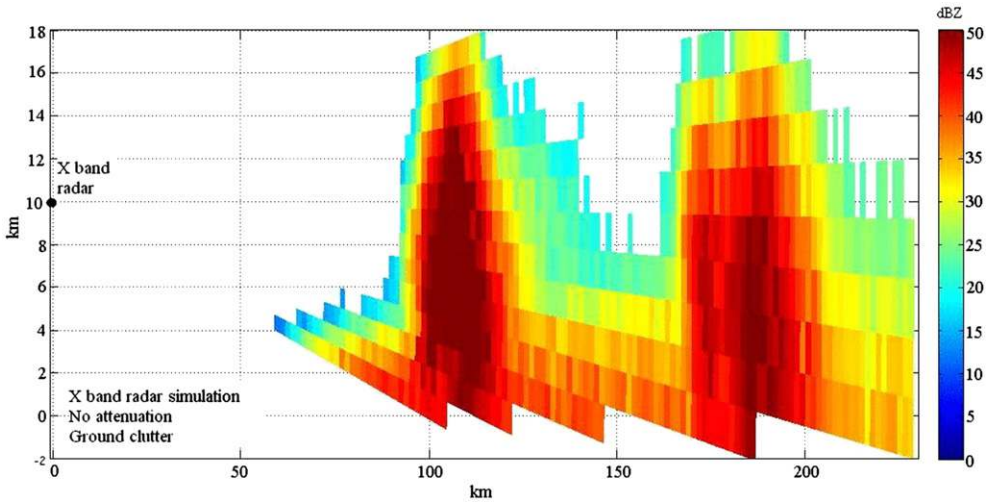

Fig. 6. Same as Fig. 4 taking into account ground clutter (attenuation is not considered in this case).

the first cell, reflectivity reaches or exceeds 40 dBZ but the horizontal extension of the core of high reflectivity is reduced and the background intercell medium is not detected.

In Fig. 6, only ground clutter is considered (attenuation is ignored). It can be seen that, due to the large aperture of the radar beam, the ground, characterized by a high reflectivity, severely contaminates the convective cells by increasing its reflectivity up to a height of about 8 km AGL. This increase is all the more important closer to the ground, where the main radar beam intercepts a large portion of the ground. This effect clearly appears between the two cells: reflectivity decreases, from 40 dBZ at the ground to 20 dBZ at a height of 8 km AGL. The combined effects of hydrometeor attenuation and ground clutter contamination appear in Fig. 7. The reflectivity field is strongly degraded. It is necessary to take into account this degradation in the interpretation of the information provided by the radar.

5. Conclusion and prospects

This work illustrates, by means of simulated radar observations, the various problems relative to thunderstorm observations at distances greater than 100 km with a X band radar of large beam aperture. This topic is of great interest for civil aviation since, for security reasons, pilots have to locate dangerous areas as soon as possible. For this study, a radar simulator using NEXRAD data at S band has been elaborated.

Three serious problems are identified and highlighted.

(1) The reflectivity field is degraded by hydrometeor attenuation at X band. Attenuation by cloud droplets is, notably, a non negligible cause of attenuation although droplets are undetected in the reflectivity field which is dominated by precipitating particles. This point has been already underlined and investigated by Pujol et al. (2007a) for cumulus clouds. The problem of cloud

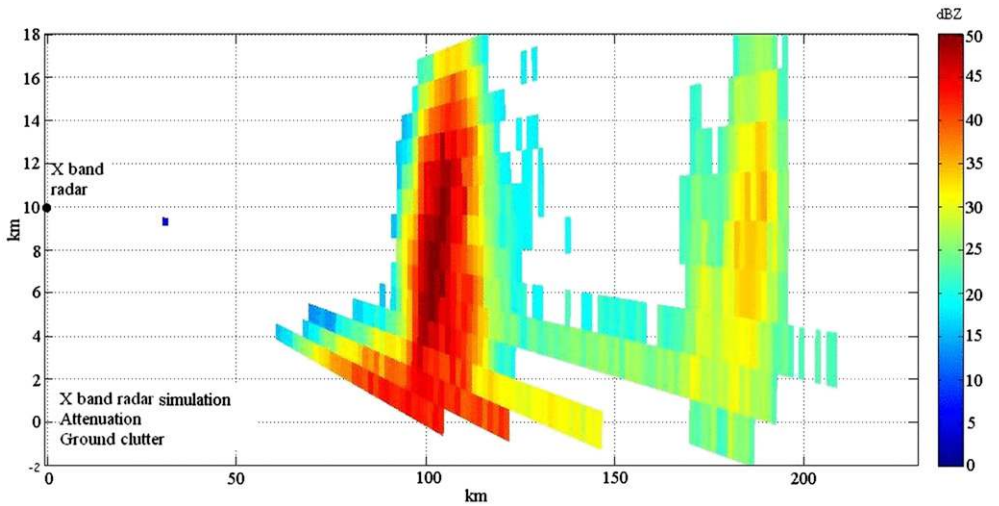

Fig. 7. Same as Fig. 4 taking into account ground clutter and hydrometeor attenuation.

droplets is all the more important because, contrary to precipitation, there is no method of correction for the cloud attenuation affecting a single wavelength non polarimetric radar.

(2) Hail detection is restricted at X band since hailstones with diameter close to or larger than the first Mie mode are difficult to identify. Indeed, such hailstones have a low radar equivalent reflectivity at X band, compared to the radar reflectivity at S band. They can be mistaken for heavy rain which is less dangerous than a hail area. This problem is crucial since a pilot would then not correctly estimate the hazard of the region the plane is heading to.

(3) Another problem arises from observations at long distances ($r > 100$ km) with a large radar beamwidth ($\theta_{3\ \mathrm{dB}} = 3°$). Since the radar beam can be as large as the size of convective cells, high reflectivity structures are smoothed by a non uniform beamfilling effect and the signal from hazards considerably weakened. Further, ground clutter strongly contaminates the reflectivity space distribution.

The importance of hazards for civil aviation justifies further studies. First, it would be necessary to find an efficient method for hail detection if X band continues to be used for meteorological airborne radar in civil aviation. Second, ground clutter and reflectivity dilution due to the large beam aperture has to be corrected as much as possible in such an observational context. Third, organization of thunderstorms in squall lines or other mesoscale convective systems should be studied. These tropical precipitating systems, which are of extreme intensity in terms of convection and precipitation, are of paramount importance for pilots. Finally, simulation should not stay in a static mode and the time component has to be added to take into account both plane motion and life cycle of convective cells.

Acknowledgments

The authors are indebted to the US NOAA/National Weather Service for providing without any charge the excellent NEXRAD network radar data used for this work.

References

Anagnostou, E.N., Krajewski, W.F., 1997. Simulation of radar reflectivity fields: algorithm formulation and evaluation. Water Resour. Res. 33, 1419–1428.
Atlas, D., Ludlam, F.H., 1961. Multi-wavelength radar reflectivity of hailstorms. Q. J. R. Meteorol. Soc. 87, 523–534.
Capsoni, C., D'Amico, M., Nebuloni, R., 2001. A multiparameter polarimetric radar simulator. J. Atmos. Oceanic Technol. 18, 1799–1809.
Doviak, R.J., Zrnic, D.S., 2006. Doppler radar and weather observations. Dover, 2nd Ed. (562 pp).
Féral, L., Sauvageot, H., Castanet, L., Lemorton, J., 2003a. A new hybrid model of the rain horizontal distribution for propagation studies: 1. Modeling of the rain cell. Radio Sci. 38. doi:10.1029/2002RS002802.
Féral, L., Sauvageot, H., Castanet, L., Lemorton, J., 2003b. A new hybrid model of the rain horizontal distribution for propagation studies: 2. Statistical modelling of the rain rate field. Radio Sci. 38. doi:10.1029/2002RS002803.
Gaussiat, N., Sauvageot, H., Illingworth, A.J., 2003. Cloud liquid water and ice content retrieval by multi-wavelength radar. J. Atmos. Oceanic Technol. 20, 1264–1275.
Giuli, D., Baldani, L., Facheris, L., 1994. Simulation and modelling of rainfall radar measurements for hydrological applications. Nat. Hazards 9, 109–122.
Glickman, T.S., 2000. Glossary of meteorology. Am. Meteor. Soc. (Boston).
Gosset, M., Sauvageot, H., 1992. A dual-wavelength radar method for ice-water characterization in mixed phase clouds. J. Atmos. Oceanic Technol. 9, 538–547.
Haase, G., Crewell, S., 2000. Simulation of radar reflectivities using a mesoscale weather forecast model. Water Resour. Res. 38, 2221–2231.
Hogan, R.J., Illingworth, A.J., Sauvageot, H., 2000. Measuring crystal size in cirrus using 35- and 94-GHz radars. J. Atmos. Oceanic Technol. 17, 27–37.
Houze, R.A., 1993. Cloud dynamics. Academic Press. (570 pp).
Klemp, J.B., 1987. Dynamics of tornadic thunderstorms. Ann. Rev. Fluid. Mech. 19, 369–402.
Mahapatra, P., 1999. Aviation weather surveillance systems. The institution of electrical engineers. (453 pp).
Nathanson, F.E., 1969. Radar design principles. Mc Graw-Hill. (626pp).
Nzeukou, A., Sauvageot, H., Ochou, A.D., Kebe, C.M.D., 2004. Raindrop size distribution and radar parameters at Cape Verde. J. Appl. Meteor. 43, 90–105.
Pruppacher, H., Klett, J.D., 1997. Microphysics of clouds and precipitation, 2nd Ed. Kluwer Academic Publishers. (943 pp).
Pujol, O., Georgis, J.F., Féral, L., Sauvageot, H., 2007a. Degradation of radar reflectivity by cloud attenuation at microwave frequency. J. Atmos. Oceanic Technol. 654–676.
Pujol, O., Georgis, J.F., Sauvageot, H., 2007b. Influence of drizzle on *Z–M* relationships in warm clouds. Atmos. Res. 86, 297–314.
Sauvageot, H., 1992. Radar meteorology. Artech House. (366 pp).
Smyth, T.J., Illingworth, A.J., 1998. Radar estimates of rainfall rates at the ground in bright-band and non-bright-band events. Q. J. R. Meteorol. Soc. 124, 2417–2434.
Vivekanandan, J., Raghavan, R., Bringi, V.N., 1993. Polarimetric radar modeling of mixtures of precipitation particles. IEEE Trans. Geosci. Remote Sens. 31, 1017–1030.